MEASUREMENT OF THE MECHANISMS OF STONE ENTRAINMENT

ROB BOOIJ

Fluid Mechanics Section (Laboratory), Faculty of Civil Engineering and Geosciences. Delft University of Technology, PO BOX 5048, 2600 GA Delft, The Netherlands, Contact:R.Booij@citg.tudelft.nl

BAS HOFLAND

Fluid Mechanics Section (Laboratory), Faculty of Civil Engineering and Geosciences. Delft University of Technology, PO BOX 5048, 2600 GA Delft, The Netherlands.

Bed protections near hydraulic structures often consist of loose granular material. The stones in these granular layers have to be stable under loads caused by flow and waves. An experimental set-up was designed in which the flow field and the pressure field were measured (by PIV and miniature pressure sensors) during the displacement of a single stone from a granular bed. From these measurements some concepts on stability could be evaluated.

Turbulence has a major influence on the entrainment of bed material. Two different kinds of turbulence-induced forces appear to play a role, the fluctuating form drag and forces resulting from pressure fluctuations. It depends on the situation which one is predominant. Several flow configurations were considered with a range of relative turbulence intensities and with a different character of the turbulent vortices: uniform flow, smooth to rough bed transition, backward-facing step (BFS) flow, and jet flow.

The exposure of stones to the flow is also seen to be very important for the relative influence of the different forces. This means that the placement of the stones is important for the stability of the bed protection.

1 Introduction

Bed protections near hydraulic structures are often composed of several layers of loose granular material (riprap). The stones in these granular layers have to be large enough to be stable under loads caused by flow and waves. In order to minimize the costs of these protections, the mechanisms that cause displacement of stones have to be known. Especially for non-uniform flow, the existing equations for stability of stones in the top layer have limited validity. The transport rate of stones under design conditions is low, with a Shields factor near the "critical" value of 0.055. This low-mobility transport is also important for gravel bed rivers (Andrews & Smith, 1992). The present measurements are therefore aimed at understanding low-mobility transport for non-uniform flows. This complicates the measurements, as the movement of the stones becomes a rare event, caused by the fluctuating forces created by the turbulence in the flow.

An elaborate measurement set-up was used to capture the flow and pressure field at the moment of entrainment of a stone from a granular bed. The measurements can aid the understanding of damage to granular bed protections and entrainment of sediments from

riverbeds. This paper focuses on the determination of the flow structures that cause entrainment.

2 Experimental set-up

2.1. *Target stone*

The experiments were executed in a flume 20 m long and 0.495 m wide. The Reynolds number was 10^5, based on the water depth h of 0.159 m and the mean bulk velocity U of 0.64 m/s. The width/depth ratio of about 3 implies the presence of some secondary flow. In this paper x and y are the streamwise and upward coordinates respectively and u and v the corresponding velocity components. The time average of u is denoted as $\bar{u}$, the fluctuating part $(u-\bar{u})$ as u', and a spatial average over area a is $\langle u \rangle_a$.

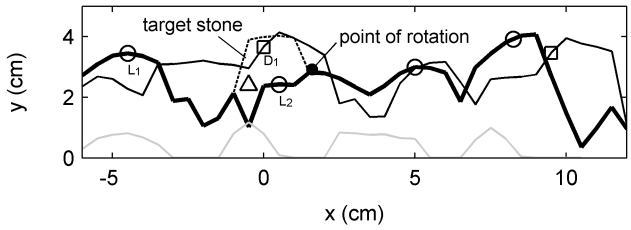

Figure 1. Measured longitudinal sections of the granular bed near the target stone indicating positions of pressure sensors (○: upward/lift, □: forward/drag, off-centre) and motion sensor (Δ). Dashed line: target stone, thick line: centre of flume, thin line: 40 mm off-centre, grey line: fixed bed. Flow is from left to right.

The experiments focussed on the movement of a single stone, the target stone. The bed material had a nominal diameter, d_{n50}, of 17.8 mm. The flow conditions that can be generated are not sufficient to move the stones. Therefore the target stone was copied with epoxy resin having a density, ρ_s, of 1300 kg/m^3. The position of the target stone and various sensors in the granular bed is depicted in figure 1. An inductive motion sensor was used to see if the stone was touching the bed. As the main mode of movement is pivoting (Carling *et al*. 1992; and our own observations), it was possible to place the stone on a hinge in such a way that the motion is the same as in the prototype situation. Further, the motion of the stone was obstructed by a little bar after pivoting over roughly 10–40 degrees, depending on the flow conditions. When the stone reaches the bar, the hydrodynamic force on the stone has increased. Therefore the stone remains pushed against the bar until it falls back with the passage of a negative fluctuation.

2.2. *Equipment*

A LaVision PIV system (hardware and software) was used to measure streamwise vertical 2D velocity fields in the centre of the flume above the target stone (Fig. 2). A sampling frequency of up to 15 Hz. was used. The flow was seeded with hollow glass spheres of 10 μm diameter. In order to diminish the bed reflections of the light sheet, the

stones under the light sheet were painted fluorescent red and an optical filter was placed in front of the camera. A vector spacing of 1.2 mm was realized. Details of the PIV set-up and data processing are given in Hofland & Booij (2004). The Kolmogorov length scale was not resolved. The unresolved fluctuations will not lead to significant forces on the stone and are therefore not of interest.

Miniature, low-range, piezo-resistive pressure transducers (Honeywell, 24PCEFA) were used to capture the pressure fluctuations near the target stone.

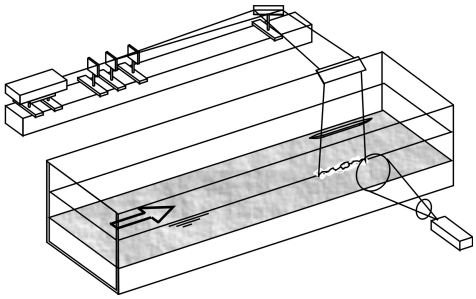

Figure 2. PIV set-up with laser (top left), sheet optics, mirrors, window on water surface and camera (bottom right).

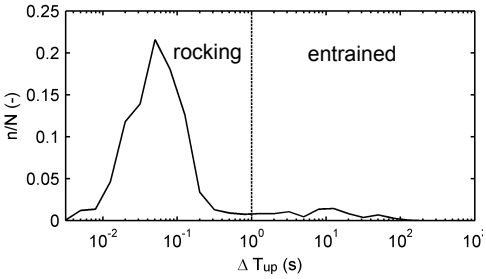

Figure 3. Histogram of the durations that the target stone is detached from the bed.

2.3. *Timing*

We discern two modes of motion of the target stone, rocking and entraining. The stone was assumed to be entrained (i.e. removed from its pocket) if it reached the obstructing bar. The fact that the stone is sometimes pushed against the bar shows up in the histogram of durations of stone motions in figure 3. If it is pushed against the bar it takes much longer for it to fall down again. This gives the small second maximum around ΔT_{up} = 10 s. The target stone was assumed to be entrained when the duration of detachment exceeded a threshold duration between the two maxima (dashed line). Otherwise the mode of movement was regarded as rocking. The threshold of one second was not strictly dividing both modes of movement, so for determination of the real entrainment events, visual inspection of the recordings was necessary.

In some cases the stone was entrained on average once every hour. Therefore the PIV and pressure measurements were only saved when the stone was regarded as entrained. The recordings were made continuously and stored in a ring buffer, so measurements could still be saved from before to after the entrainment. When the stone did fall back eventually, a new recording started automatically when the prior data were saved and the stone was back in its original position.

2.4. *Flow configurations*

Several flow configurations were considered with a range of relative turbulence intensities and with a different character of the turbulent vortices:

(1) A **uniform flow**, which has low turbulence intensity. The turbulence was considered fully developed with the rough bed spanning a length of 66 water depths, h, upstream of the target stone. The flow comprises large-scale sweep motions (length ≈ several h) bordered by small-scale hairpin/horseshoe vortices (length ≈ d) originating at the bed.
(2) A **smooth bed to rough bed transition**, which shows underdeveloped low-frequency turbulence. The large-scale sweeps have not fully developed here.
(3) A **backward-facing step** (BFS) flow, with increased turbulence intensity at the reattachment point. The eddy behind the step shows low-frequency motions and intense 2D rollers that originate in the mixing layer, which turn into energetic hairpin/horseshoe-vortex packets downstream of the reattachment point.
(4) A **jet flow**, which has spanwise vortices rotating in the opposite direction compared to the BFS. The relevance of turbulent pressures and velocities on jet flow erosion is outlined more in detail in an accompanying paper (Bollaert & Hofland, 2004).

3 Physical concepts of stability

We previously identified two force-generating mechanisms that may be responsible for the entrainment of stones (Hofland & Booij, 2004; Hofland *et al.*, to be publ.).

- Quasi-steady force fluctuations (QSF), caused by large-scale motions ($u'>0$, and usually $v'<0$).
- Small-scale turbulence wall pressure fluctuations (TWP), caused by small-scale wall-normal fluctuations (v') and vortices.

We use the actual movement of a stone as a trigger to distinguish the velocity fields leading to stone entrainment. Then we divide the flow fields for all events into two classes, corresponding to these entrainment mechanisms. Next we describe how we can distinguish the different kinds of flow structures that cause entrainment.

3.1. *Quasi-steady forces*

Most stability formulae that incorporate turbulent fluctuations regard the streamwise velocity near the bed (or the shear velocity u_*). This is based on the fact that the steady drag and lift force vary according to $|u|u$ and u^2. So a fluctuation of u will lead to quasi-steady fluctuating forces (QSF). To quantify the influence of this force-generating mechanism we average the instantaneous u-velocity in the PIV recordings over an area A above the stone, yielding $\langle u \rangle_A$, and regard the values of $F_A \propto |\langle u \rangle_A| \langle u \rangle_A$ and its fluctuations.

3.2. *Turbulence wall pressures*

A turbulent flow over a bed creates wall pressure fluctuations (TWP) on this bed, even if it is smooth. These pressures can also lead to net forces on bed material (Hofland & Booij, 2004). The origin of intense TWP can be vortices (e.g. Müller *et al.*, 1971). As only TWP with a length scale of the order of the stone diameter d will give significant

forces on a stone, a vortex at 0.5–2*d* above the target stone will induce a large (lift) force. The force vector rotates clockwise from a lift to a drag direction as the vortex passes. This lift-drag combination could be efficient in starting the entrainment. To identify the presence of this force-generating mechanism we regard the spatial standard deviation, $\sigma(v)_B$, of v over an area B around the target stone. The value of $\sigma(v)_B$ becomes large when a vortex is present, and is not very sensitive to the exact position of the vortex.

Another good indicator for the presence of vortices is the swirling strength, λ_{ci}. This is the imaginary part of the complex eigenvalues of the shear tensor. In a 2D flow this is equal to the source term for pressure, $-Q$, which is present in the Poisson equation, $\nabla^2 p = 2\rho Q$. This also shows that the presence of a vortex indicates the presence of a pressure gradient, which can lead to the entrainment of a stone.

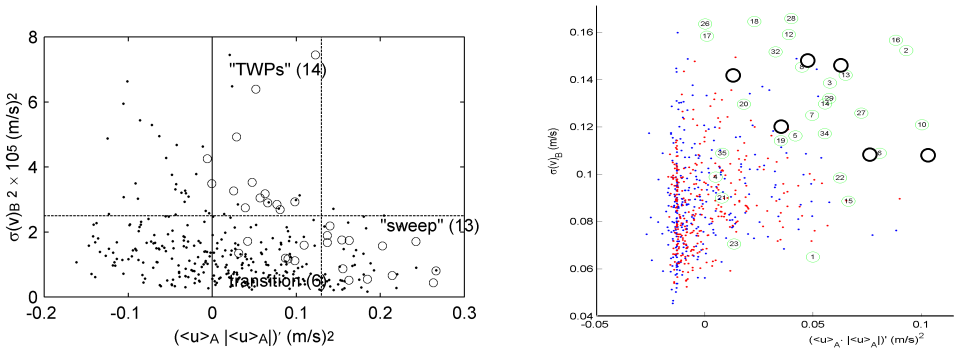

Figure 4. Classification of events: $|\langle u\rangle_A|\langle u\rangle_A$ and $\sigma(v)_B$ indicate quasi-steady and TWP forces respectively. Left: a uniform flow and right: a BFS flow. Dots are the values of a measurement with a fixed stone. The circles are the values just before an entrainment event.

4 Results

We now regard the measured flow fields during stone movement and see whether the indicators for the quasi-steady and TWP forces are increased at these times. Figure 4 shows the values of the indicators. It is obvious that both indicators are high at the time of movement, compared to an average recording – both for the uniform and the BFS flow. We can thus infer that both the TWP and the QSF aid in the initiation of movement in the uniform and BFS cases.

The TWP-forces are sometimes related to strong vortices, see figures 5 and 6. At 7 of the 33 entrainment events of the uniform flow an obvious vortex was visible. At 8 other we saw a packet with several smaller vortices aligned. We must also keep in mind that we can only see vortices that are oriented roughly in the spanwise direction.

The sweep movements can become very large. The average sweep shown in figure 5 is already roughly 5*h* long.

The intensities of the two force-mechanisms are inversely proportional. The circles representing the entrainment events in figure 4 form a declining line. This means that if one mechanism is very strong, the other does not need to be very strong in order to have

a combined force strong enough for the initiation of movement. Figure 5 shows conditionally averaged plots of both the events with large quasi-steady forces and with large TWP forces. They confirm that the sweep-dominated events show a large sweep with a small vortex, and TWP-dominated events show an increased λ_{ci} inside a smaller sweep.

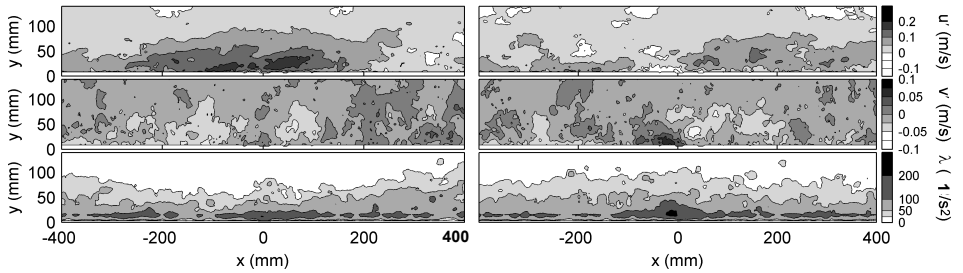

Figure 5. Conditionally averaged large-scale flow field (u', v' and λ_{ci}) for uniform flow at the moment of entrainment. Left: sweep dominated. Right: TWP-dominated. h = 0.16 m. Target stone is positioned at (0,0).

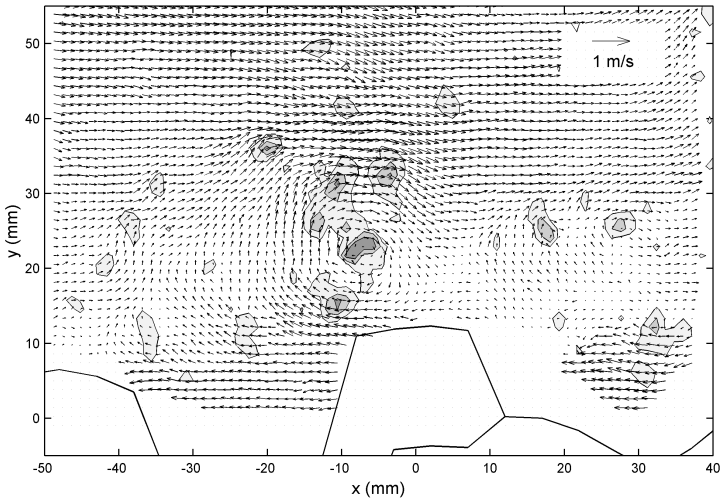

Figure 6. Detail of an instantaneous flow field in uniform flow just before stone movement. Vectors: $\vec{u} - 0.65U$. Shading: λ_{ci}.

From the pressure measurements we saw that at the beginning of the rough bed the large-scale sweeps are less developed and less intense than for the uniform flow, causing decreased forces at low frequencies, and hence leading to less damage.

For the uniform and BFS cases the vortex is usually rotating clockwise. This leads to a decreased QSF at times of increased TWP. Therefore we see that the vortices are embedded in a large-scale sweep. This gives a sequential occurrence of TWP and quasi-

steady forces: first the vortex gives the stone its first lift, then the sweep transports the stone further.

In case of jet flow most vortices rotate counter-clockwise, which makes them more efficient, as both the quasi-steady force and the TWP are increased simultaneously with the presence of a vortex (Bollaert & Hofland, 2004).

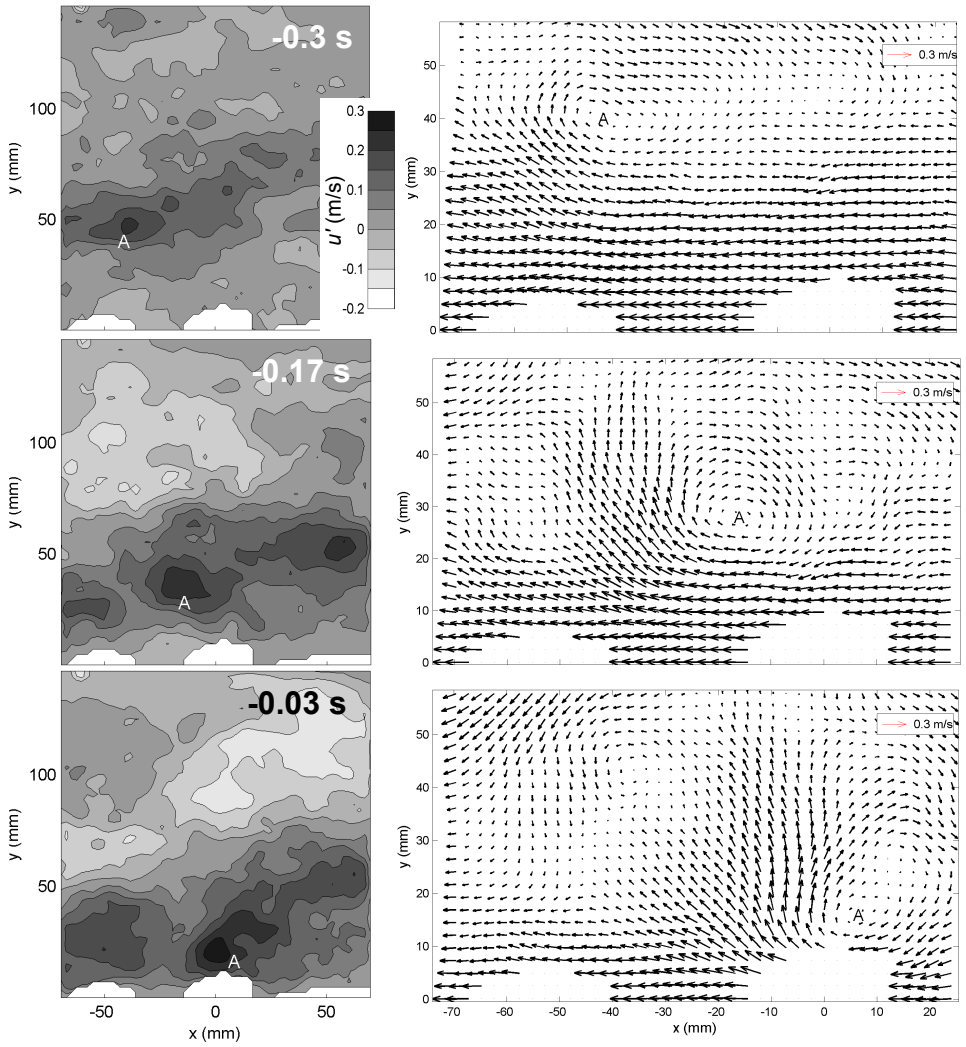

Figure 7. Conditionally averaged flow field around the reattachment point behind a BFS, at different times (0.3, 0.17, 0.03 s) before stone entrainment. The stone is positioned at (0,0). Left: contour plots of u'. Right: vector plots of $\vec{u} - 0.8U$ (detail). Point A indicates the position of the flow structure that moves the stone. (Courtesy: R. de Ruijter)

In the conditionally averaged flow fields just before movement in a BFS flow (figure 7) a Q4 event ($u'<0$, $v'>0$) just upstream of the vortex A indicates that this is the head of a hairpin/horseshoe vortex. The Q4 event is the flow induced by the legs of this vortex, which are not directly visible. The large-scale patch of increased u in which the vortex is embedded is probably due to the flapping of the recirculation zone.

5 Conclusions

Turbulence has a major influence on the entrainment of bed material. Two different kinds of turbulence-induced forces appear to play a role, the fluctuating form drag (QSF-mechanism) and forces resulting from pressure fluctuations (TWP-mechanism).

Indicators for both mechanisms were developed. The near-bed u' indicates the presence of quasi-steady force fluctuations (QSF), and the near-bed $\sigma(v)$ and λ_{ci} indicate TWP-induced forces. The behaviour of the indicators was investigated for several flow configurations. It was observed that it depends on the situation which mechanism is predominant. Often both mechanisms act together in the entrainment of a stone.

Acknowledgements

The research has been financially supported by the Road and Hydraulic Engineering Division of the Ministry of Transport, Public Works, and Water Management, (contract DWW-1700) and by Delft Cluster, under the theme Coast and River.
The authors wish to express their thanks to mr. R. de Ruijter for his precision and stamina during the measurements and data-analysis of the BFS flow.

References

Andrews, E.D. and Smith, J.D. (1992). "Theoretical model for calculating marginal bedload transport rates of gravel." In Billi, P. Hey, C.R. Thorne, C.R. and Tacconi, P. (eds), *3rd int. workshop on dynamics of gravel-bed rivers*, New York: John Wiley & Sons

Bollaert, E. and Hofland, B. (2004). "The influence of turbulence on particle movement due to jet impact." *Int. Conference on Scour and Erosion 2004, Singapore*.

Carling, P.A. Kelsey, A. and Glaister, M.S. (1992). "Effect of Bed Roughness, Particle Shape and Orientation on Initial Motion Criteria." In Billi, P. Hey, C.R. Thorne, C.R. and Tacconi, P. (eds), *3rd int. workshop on dynamics of gravel-bed rivers*, New York: John Wiley & Sons

Hofland, B. and Booij, R. (2004). "Measuring the flow structures that initiate stone movement." *Proc.River Flow 2004, 2nd Int. Conf. on Fluvial Hydr., Naples, Italy.*

Hofland, B. Booij, R. Battjes, J.A. (to be published). "Measurement of fluctuating pressures on coarse bed material." *J. Hydraulic Eng.*

Müller, A., Gyr, A., and Themistocles, D. (1971). "Interaction of rotating elements of the boundary layer with grains of a bed; a contribution to the problem of the threshold of sediment transportation." *J. Hydr. Research* 9(3).